Equalization Algorithm for Distributed Energy Storage Systems in Islanded AC Microgrids

Aldana, Nelson Leonardo Diaz; Hernández, Adriana Carolina Luna; Quintero, Juan Carlos Vasquez; Guerrero, Josep M.

Published in:
Proceedings of the 41th Annual Conference of IEEE Industrial Electronics Society, IECON 2015

DOI (link to publication from Publisher):
10.1109/IECON.2015.7392827

Publication date:
2015

Document Version
Accepted author manuscript, peer reviewed version

Equalization Algorithm for Distributed Energy Storage Systems in Islanded AC Microgrids

Nelson L. Díaz*†, Adriana C. Luna*, Juan C. Vásquez*, and Josep M. Guerrero*
*Department of Energy Technology, Aalborg University, Aalborg, Denmark
†Faculty of Engineering, Universidad Distrital F. J. C., Bogotá, Colombia
nda@et.aau.dk, acl@et.aau.dk, juq@et.aau.dk, joz@et.aau.dk
www.microgrids.et.aau.dk

***Abstract*—This paper presents a centralized strategy for equalizing the state of charge of distributed energy storage systems in an islanded ac microgrid. The strategy is based on a simple algorithm denoted as equalization algorithm, which modifies the charge or discharge ratio on the time, for distributed energy storage systems, within a determined period of time in order to equalize the state of charge. The proposed approach has been tested in a MATLAB/Simulink model of the microgrid where the performance of the proposed strategy was verified.**

***Keywords*—Distributed energy storage systems, Droop control, Equalization algorithm, State of Charge.**

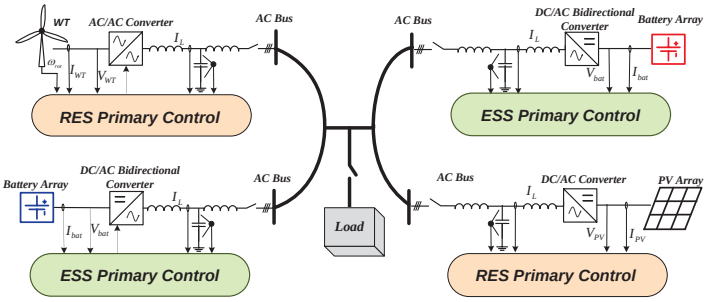

Fig. 1: Islanded AC microgrid configuration.

I. Introduction

A microgrid is an integration of distributed energy resources, loads and energy storage units into a controllable system, which is able to operate either in grid connected or islanded mode [1]. Particularly, islanded microgrids play an important role when economic and environmental issues do not allow interconnection with the main power grid [2]. Nowadays, renewable energy sources (RES) such as photovoltaic and wind turbine generators have been widely used in order to replace traditional coal, oil and other non-renewable energy resources. Consequently, energy storage systems (ESS) have become an indispensable element into a microgrid based on RES units for smoothing the intermittent nature of RES's [3].

As a matter of fact, the current trend is oriented to distributed ESS's instead of aggregated ESS's. To be more precise, an ESS is associated to each RES integrated into a microgrid. As a result, more redundancy, energy support, and constant power production can be ensured when RES are used [4]–[7]. Valve regulated lead-acid (VRLA) batteries are commonly used in islanded microgrids, since they offer a good commitment between deep-cycle life, transportability, availability and cost [7], [8]. Fig. 1 shows the basic scheme of an islanded microgrid composed by two RES, two ESS's and the load.

On top of that, when distributed ESS's are used, it is required coordinated operation between them in order to avoid deep-discharge in one of the energy storage unit and over-charge in the others. Differences at the SoC could limit the life-time of the ESS with the smallest SoC, since this ESS will be exposed to bigger deep of discharge [9]. Therefore, when the ESS's are charged, it is desirable to prioritize the charge of the unit with the smallest state of charge (SoC). On the contrary, when the ESS's are discharged, the unit with the highest SoC should provide more power to the microgrid than the others in order to ensure stored energy balance [10], [11].

Commonly, droop control strategies are used in order to achieve power sharing between units [12]. Therefore, conventional control loops for power sharing at each ESS is complemented with adaptive strategies which adjust the droop coefficients in accordance to the SoC. In this way, it is possible to reach asymptotic approach of the SoC. At this sense, several different approaches have been proposed for equalizing the SoC at distributed ESS's such as in [6], [7], [13]–[19]. However, all of them have been applied to dc microgrids. In addition, equal capacity is assumed for all the distributed ESS. Besides, the equalization time is very sensitive to the parameters of the equalization functions. Because of this, the stability of the system can be compromised when shorter equalization times are sought. Another approach which considers differences at the capacity of the energy storage unit is presented in [6]. In this case, the ESS's are based on electric-double-layer capacitors rather than on batteries. Although, the stored energy is balanced, long time and additional control loops are required.

This paper proposes a new function for the energy management system (EMS) of an islanded ac microgrid based on a centralized equalization algorithm which achieves asymptotic approach of the SoC at distributed ESS based on batteries. The proposed equalization algorithm weights the droop coefficients of the droop control loops, within a defined window of time, in order to obtain asymptotic approach of the SoC. The adaptive value of the droop coefficients is bounded what ensures the stability of the microgrid. Simulation results in a MATLAB/Simulink model of the microgrid show the effectiveness of the proposed model even under differences at the capacity of each ESS.

It is important to say that this paper will only consider the operation of the microgrid when the ESS's are being charged or discharged. Anyhow, the operation of the microgrid should be complemented by appropriate charge strategies that avoid excessive overcharge in the batteries, such as in [7], and [19], as well as load-shedding, or actions for limiting the deep of discharge of the batteries as proposed in [20].

The paper is organized as follows. Section II explains the operation of the microgrid and how conventional droop control loops are adjusted in order to obtain equalization of SoC. After that, section III presents the centralized equalization algorithm, and finally sections IV and V present simulation results and conclusions respectively.

II. Droop Control Loop Adjustment

Normally, in an islanded microgrid all the primary controllers are typically set up to operate in voltage control mode (VCM) by following conventional droop control strategy. In this way, it is possible to regulate the bus voltage and frequency and achieve good power sharing between units [12]. Even though, this approach is not the most advisable for intermittent sources such as RES units, which are more likely to operate under algorithms of maximum power tracking (MPPT) in order to obtain from them the maximum amount of available energy.

Because of this, RES units assume the role of grid-following units, behaving as current sources and their primary controllers are set up to operate on current control mode (CCM) [20], [21]. Consequently, the ESS units assume the role of grid-forming units operating in VCM being the responsible of regulating the ac bus. Meanwhile, they will be charged or discharged in order to compensate the power unbalance between the generated and consumed power [19].

When the ESS units are in the process of charge or discharge, the power balance is managed by $P-\omega$ droop control loops [12]. Therefore, the frequency at the common ac bus is established by the following equation,

$$\omega = \omega^* - m_0 \cdot P_{Bati} \tag{1}$$

where m_0 is the droop coefficient, ω is the angular frequency at the common bus, ω^* is the reference of the angular frequency, P_{Bati} is the active power at each i-th ESS unit ($i = [1, \cdots, n]$) and n is the number of distributed active generators (RES+ESS)). When the same droop coefficient (m_0) is applied to each ESS unit, the power is shared equally between ESS units as we can see in Fig. 2a.

Under the discharge process, for balancing the SoC, the ESS with the highest SoC should supply more power to the microgrid than the others. On the other hand, when the ESS units are being charged, the ESS with the smallest SoC should get more energy from the microgrid than the others. This behavior can be achieved by weighting the droop coefficient (m_0) by a factor α_i as is shown in Fig. 2b and Fig. 2c for discharge and charge of ESS units respectively. In the case of Fig. 2b and Fig. 2c it is assumed that $SoC_{Bat2} > SoC_{Bat1}$. In the figures, it is possible to see that for the charging process $|P_{Bat1}| > |P_{Bat2}|$. On the contrary, for the discharging process $|P_{Bat2}| > |P_{Bat1}|$, this characteristic has to be taken into account when the weighting factors α_i are determined. To get back to the point, equation (1) is now rewritten as follows

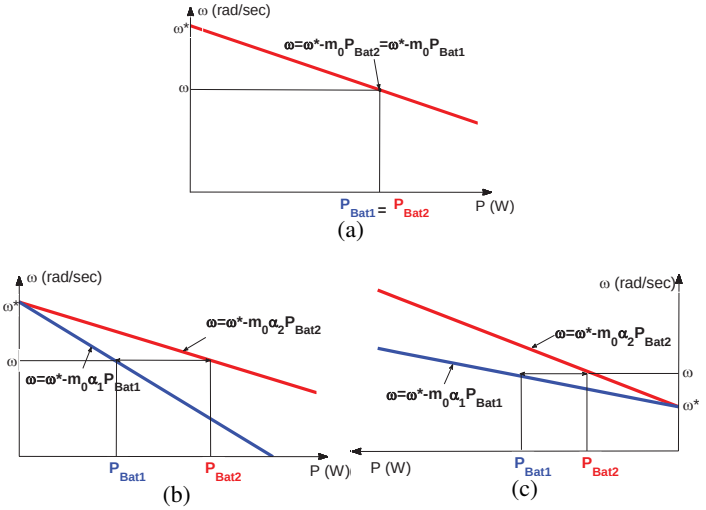

Fig. 2: Active power sharing: (a) for equal droop coefficients, (b) weighted droop coefficients for ESS discharging, (c) weighted droop coefficients for ESS charging.

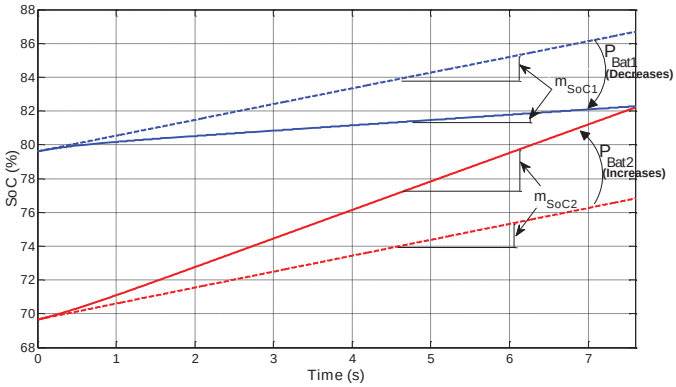

Fig. 3: Expected behavior of the equalization algorithm.

$$\omega = \omega^* - m_0 \cdot \alpha_i \cdot P_{Bati} \tag{2}$$

III. Equalization Algorithm

The algorithm is based on the fact that the rate of change of the SoC is directly proportional to the battery power

$$P_{Bati} \propto m_{SoCi} \tag{3}$$

where m_{SoCi} is the rate of change for the SoC at each ESS. For that reason, by adjusting m_{SoCi} it is possible to achieve an equalization of the SoC at distributed ESS as is shown in Fig. 3.

First of all, the SoC at each ESS is estimated by ampere-hour (Ah) counting method

$$SoC(\Delta t)_{Bati} = SoC(0)_{Bati} - \int_0^{\Delta t} \eta_{Bati} \frac{I_{Bati}(\tau)}{C_{Bati}} d\tau \tag{4}$$

where $SoC(0)_{Bati}$ is the initial SoC, C_{Bati} is the capacity in (A/h), η_{Bati} is the charging/discharging efficiency, and $I_{Bati}(\tau)$ is the instantaneous current at each battery array [8].

By considering a constant current charge, the power at each battery array can be approximated as

$$P_{Bati} \approx V_{Bati} * I_{Bati} \tag{5}$$

where (V_{Bati}) is the nominal voltage of the battery array. Despite this approximation is not accurate, it provides us enough information about the battery capacity at every ESS. Then, from (4) and (5), it is possible to obtain

$$P_{Bati} \approx -\frac{\Delta SoC_{Bati}}{\Delta t}\left(\frac{V_{Bati}C_{Bati}}{\eta_{Bati}}\right) \approx -m_{SoCi}K_{Bati} \tag{6}$$

where, m_{SoCi} is the rate of the SoC, and K_{Bati} is a proportionality constant that depends on the main parameters of the ESS.

In a general case, where n distributed active generators (RES+ESS) are integrated into the microgrid, it is easy to derive the power balance equation as:

$$\sum_{i=1}^{n} P_{Bati} + \sum_{i=1}^{n} P_{RESi} - P_{load} = 0 \tag{7}$$

where P_{load} is the load consumption, and P_{RESi} is the power supplied for each RES. Combining (6) and (7), we have:

$$\sum_{i=1}^{n} -m_{SoCi}K_{Bati} + \sum_{i=1}^{n} P_{RESi} - P_{load} = 0 \tag{8}$$

When an equalization of the SoC is required within a defined period (Δt), $SoC(\Delta t)_{Bat(i-1)} = SoC(\Delta t)_{Bati} = SoC(\Delta t)_{Bat(i+1)}$. Because of this, the straight-line equation of a particular i-th ESS unit can be equalized with the straight-line equation of other i-th ESS unit as

$$SoC(0)_{Bati} + m_{SoCi}\Delta t = SoC(0)_{Bat(i+1)} + m_{SoC(i+1)}\Delta t \tag{9}$$

Reorganizing the equation system formed by expressions (8) and (9), we can derive the following symbolic matrix representation as

$$[A][X] = [B] \tag{10}$$

where, $[A] = (a_{e,v})_{nxn}$ and

$$a_{e,v} = \begin{cases} -K_{Bati}, & \textbf{If } e = 1 \ \ \& \ \ v = i; \\ \Delta t, & \textbf{If } e = i+1 \ \ \& \ \ v = i; \\ -\Delta t, & \textbf{If } e = i+1 \ \ \& \ \ v = i+1; \\ 0, & \textbf{Otherwise} \ . \end{cases} \tag{11}$$

is the entry in the e-th row and v-th column of A.

$$[X] = [m_{SoC1}, m_{SoC2}, \cdots, m_{SoCn}]^T \tag{12}$$

$$[B] = \begin{bmatrix} -(\sum_{i=1}^{n} P_{RESi} - P_{load}) \\ (SoC(0)_{Bat2} - SoC(0)_{Bat1}) \\ \vdots \\ (SoC(0)_{Batn} - SoC(0)_{Batn-1}) \end{bmatrix} \tag{13}$$

Consequently, the adequate values for each m_{SoCi} that ensure the equalization of the SoC within a defined period of time (Δt) can be obtained as

$$[X] = [A]^{-1} \times [B] \tag{14}$$

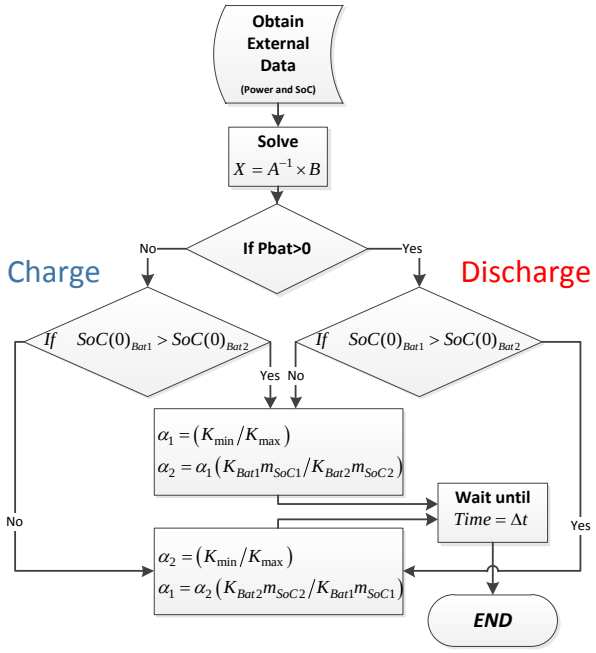

Fig. 4: Equalization algorithm diagram.

The main task of the equalization algorithm is to solve the equation (14), in order to obtain the values of m_{SoCi}. Once the value for each m_{SoCi} is calculated, the weighting factor α_i in (2) is obtained for each ESS droop control loop in accordance to:

$$\alpha_1 \cdot P_{Bat1} = \alpha_2 \cdot P_{Bat2} = \alpha_i \cdot P_{Bati} \tag{15}$$

Then, the next step in the algorithm is to identify if the ESS's are being charged or discharged. Afterwards, it is necessary to identify which ESS has the biggest value of SoC. The idea is to weight the nominal droop factor m_0 in accordance to the SoC and battery array capacity. To be more precise, during the operation of the algorithm, when the ESS units are being charged, the largest weight is assigned to the ESS unit with the biggest value of SoC. This maximum weight is defined by (K_{min}/K_{max}), where K_{min} and K_{max} are the minimum and maximum values of the proportionality constant defined in (6). In this way, it is ensured that the droop coefficient $(\alpha \cdot m_0)$ will never be bigger than its nominal value, what avoids under-damped behaviors in the response of the microgrid [22]. On the contrary, for the process of discharging the ESS's, the largest value of the weighting factor will be assigned to the ESS unit with the lowest SoC. To illustrate, the algorithm for two active generators based microgrid ($n = 2$) is summarized in Fig. 4, where the initial step of the centralized algorithm is to obtain the external data from the distributed units.

Since the proposed algorithm is based on simple matrix operation, the computational time is very small (around $0.15s$). This time can be negligible compared with the time scale required for charging batteries (normally hours).

Apart from that, since the equalization is only defined during a specified period, it is required to define how the weighting factor will be established during periods of no equalization. In this case, a similar charge/discharge rate is expected for each i-th ESS, this is ($m_{SoCi-1} = m_{SoCi} = m_{SoCi+1}$).

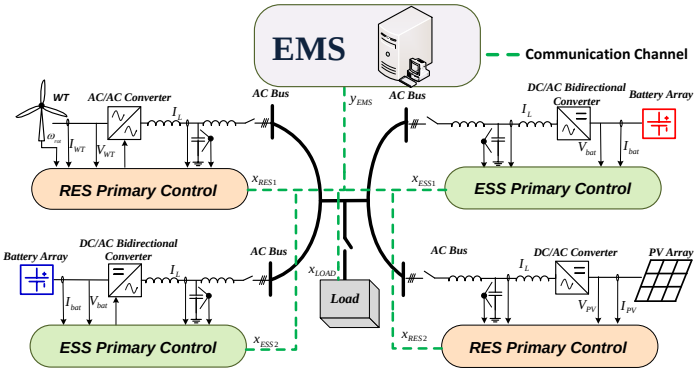

Fig. 5: Diagram of the AC islanded microgrid with centralized EMS.

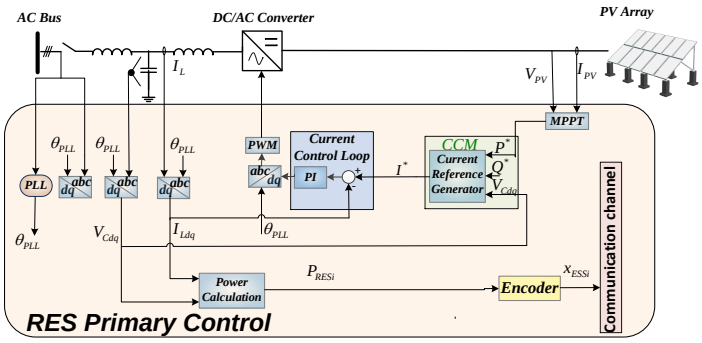

Fig. 6: Control diagram for RES.

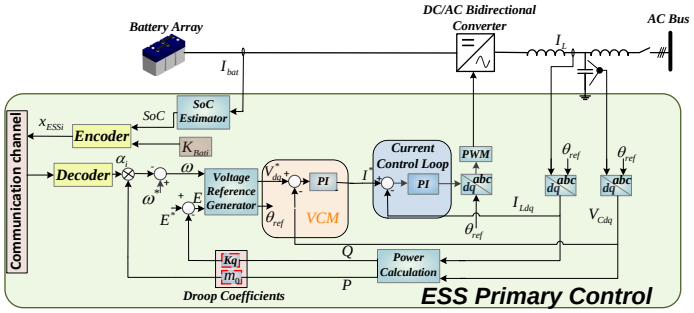

Fig. 7: Control diagram for ESS.

This is also the behavior expected once the SoC's have been equalized. Regarding differences at the ESS's capacities, the largest value of the weighting factor ($\alpha_i = 1$) will be assigned to the ESS with the smallest capacity. Meanwhile, the others ESS units will get a weighting factor in accordance to:

$$\alpha_i = \frac{K_{min}}{K_{Bati}} \tag{16}$$

IV. Operation of the Microgrid

The general scheme of the microgrid considered for this study is composed by two RES generators (a photovoltaic (PV) generator and a wind turbine (WT) generator), two ESS units based on batteries, a critical load, a centralized EMS for performing the equalization algorithm and a dedicated full-duplex communication channel as can be seen in Fig. 5. User Datagram Protocol (UDP) is used for interchanging data between each distributed energy unit and the EMS.

The data sent from each RES unit (X_{RESi}), each ESS unit (X_{ESSi}), and the load (X_{LOAD}) are set as

$$X_{RESi} = [P_{RESi}] \tag{17}$$

$$X_{ESSi} = [K_{Bati}, SoC_{Bati}]^T \tag{18}$$

$$X_{LOAD} = [P_{load}] \tag{19}$$

The data sent from the EMS to each RES unit Y_{EMS}, is just the weighting factor (α_i)

$$Y_{EMS} = [\alpha_i] \tag{20}$$

As aforementioned, in islanded operation for charging/discharging process of the ESS units, the RES units assume the role of grid-following units operating under (CCM) inner loop that follows maximum power point tracking (MPPT) algorithm. MPPT strategies are out of the scope of this paper, interested readers may also refer to [23] and [24]. To get back to the point, the inductor current of the converter is controlled by typical inner current loops. Fig. 6 shows the scheme of the inner current control for a RES based on PV generator. In general, the control scheme for a RES based on WT is the same as shown in Fig. 6 taking into account differences at the power converter and MPPT method [24].

Meanwhile, the ESS operate in voltage control mode (VCM) being responsible of regulating the bus voltage. At this mode, the batteries will be charged or discharged in order to compensate the unbalance between the energy generated by RES and load consumption [19], [13]. The power unbalance is shared between ESS by means of conventional droop control loop adjusted by the weighting factor α_i in order to achieve SoC equalization. In this case, a typical double-loop VCM controller is implemented for a bidirectional inverter, as can be seen in Fig. 7. The reactive power flow Q is equally shared between distributed ESS in accordance to conventional $Q-E$ droop control loops as

$$E = E^* - K_q \cdot Q \tag{21}$$

where, E is the voltage amplitude of the inverter, Q is the reactive power at the respective unit, E^* is the voltage reference and K_q is the droop coefficient [25].

The microgrid has been designed to supply a nominal resistive load in a balanced three phase system. An aggregated model based on a detailed model of a VRLA battery array, proposed in [7] has been used for simulating the batteries. Table I summarizes the main parameters of the microgrid.

V. Results and Discussion

A MATLAB/Simulink model of the ac microgrid has been used in order to test the operation of the equalization algorithm. The microgrid is composed by a PV, a WT, the communication channel and their corresponding ESS as is shown in Fig. 5.

Three main cases have been considered for the evaluation of the equalization algorithm. Those are, $C_{Bat1} = C_{Bat2}$, $C_{Bat2} > C_{Bat1}$, and $C_{Bat2} < C_{Bat1}$. All the cases were

TABLE I: Main Parameters of the Microgrid

Parameter	Value
Nominal Bus Frequency (ω^*)	$2 * \pi * 50$ (rad/sec)
Nominal Bus Voltage (E^*)	$230 * \sqrt{2}$ (V)
Nominal Load	1600 (W)
Maximum (RES) Power Rating	2200 (W)
Nominal Battery Voltage (V_{Bat})	672 (V)
Charging/discharging efficiency (η_{Bati})	93%
Nominal Battery Capacity (C_{Bat})	0.02 (Ah)
Period of the Equalization Algorithm (Δt)	5 (sec)
Nominal Droop Coefficient (m_0)	$1.25 * 10^{-5}$ (rad)/(sec)/(W)
$(Q - E)$ Droop Coefficient (K_q)	$5 * 10^{-4}$ V/(VAr))
Reactive power Reference (Q^*)	0 (VAr)

implemented by considering a total generation from RES of $P_{RES1} + P_{RES2} = 3000W$ and $P_{RES1} + P_{RES2} = 0W$ for charging and discharging respectively. Particularly, small values of capacity ($C_{max} = 0.02Ah$) have been selected in order to speed up the simulation time. For simulation purpose, the equalization will be activated at 5 and 15 s for a period $\Delta t = 5s$. Therefore, we can also see the behavior of the system during periods of no equalization. In general the time for running the equalization can be adjusted in accordance to the requirements of the EMS.

A. Case $C_{Bat1} = C_{Bat2}$

Fig. 8a shows the performance of the equalization algorithm when the ESS's are being charged. An initial SoC of 55% and 65% have been established for ESS1 and ESS2 respectively. Fig. 8a shows the equalization process for SoC_{Bat1} and SoC_{Bat2}, the active power at each ESS unit where we can see how the power is shared and adjusted during the equalization in order to achieve the objective. At the end, Fig. 8a shows the difference between SoC

$$Diff(SoC) = SoC_{Bat2} - SoC_{Bat1} \tag{22}$$

where, it is possible to see that the difference is practically zero after two iterations. Similarly, Fig. 8b shows the response of the microgrid when the ESS's are being discharged. In this case, an initial SoC of 85% and 95% have been established for ESS1 and ESS2 respectively. Comparing Fig. 8a and Fig. 8b during the equalization, we can see that for the discharging process $|P_{Bat2}| > |P_{Bat1}|$. Meanwhile, for the charging process $|P_{Bat1}| > |P_{Bat2}|$. We can also see in Figs. 8a and 8b that the power is equally shared during periods of no equalization (10s to 15s) and (20s to 25s), since both ESS have the same capacity.

B. Case $C_{Bat2} > C_{Bat1}$

Fig. 9a and 9b show the response of the microgrid when $C_{Bat1} = 0.01(A/h)$. Similar initial conditions to the previous case have been established. We can see that when the equalization is not applied (10s to 15s, and 20s to 25s), we have $|P_{Bat2}| > |P_{Bat1}|$. The reason of this is that ESS2 requires much more power in order to achieve $m_{SoC1} = m_{SoC2}$. However, when the algorithm is applied, the current is adjusted in order to equalize the SoC's.

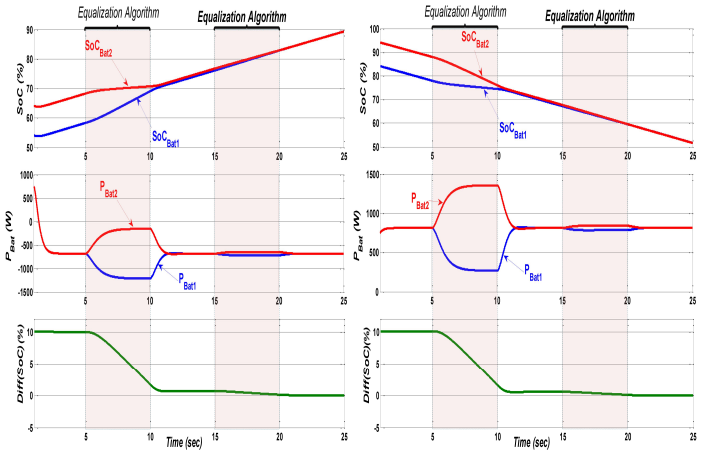

(a) (b)

Fig. 8: Case $C_{Bat1} = C_{Bat2}$: (a) Charge (b) Discharge.

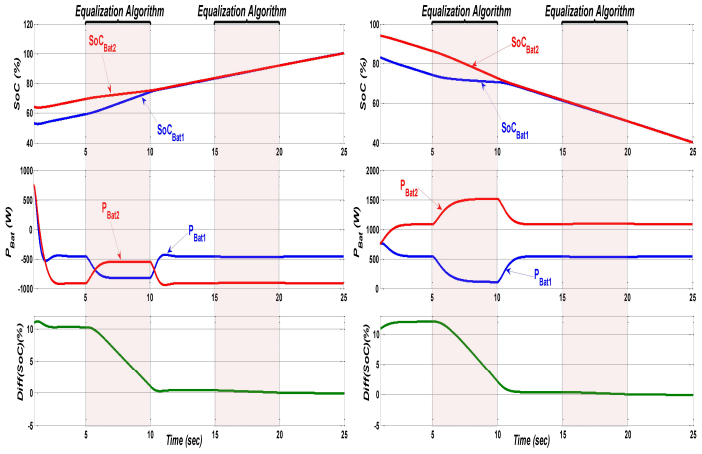

(a) (b)

Fig. 9: Case $C_{Bat1} < C_{Bat2}$: (a) Charge (b) Discharge.

C. Case $C_{Bat2} < C_{Bat1}$

Fig. 10a and 10b show the response of the microgrid when $C_{Bat2} = 0.01(A/h)$. Compared to the previous case, $|P_{Bat2}| < |P_{Bat1}|$, when the equalization is not applied.

We can see how the difference is reduced when the algorithm is applied. Nevertheless, they are required two iterations of the equalization algorithm in order to reach $Diff = 0$, this is because the transitory and dynamic response have not been considered by the algorithm. Apart from that, the approximation in (5) can lead to small errors in the equalization process. Nevertheless, the proposed approach has proved to be faster and more accurate for the equalization of the SoC compared to other approaches such in [4], [17]–[19]. Additionally, for the proposed approach, we have considered differences at the capacities of the distributed ESS's, and the equalization is ensured despite the differences. Moreover, one of the main advantages of the proposed method is that it is based on simple algebraic operations what makes its processing time very small (less than 160 ms).

VI. Conclusion

The proposed strategy has demonstrated to be effective for SoC equalization in distributed ESS's. Despite, they were

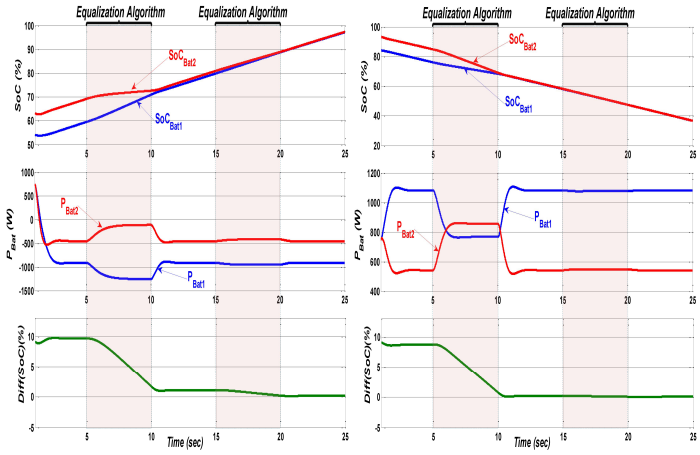

(a) (b)

Fig. 10: Case $C_{Bat1} > C_{Bat2}$: (a) Charge (b) Discharge.

established several approximations for defining the model and transitory response is not considered by the algorithm (linear behavior is assumed), the algorithm is able to equalize the SoC within few iterations. This algorithm can be complemented by an optimization process in order to minimize the period of time Δt, and more accurate models can be evaluated. Additionally, power constraints should be taken into account for the optimization by considering the maximum power ratings of the ESS's. On the other hand, for a complete operation of the islanded microgrid, it is necessary to consider a adequate architecture for the operation of the microgrid which considers changes at the operation mode of batteries or curtailment of RES's generation when batteries are fully charged. As well as consider load shedding strategies for avoid deep discharge of batteries.

REFERENCES

[1] J. Vasquez, J. Guerrero, J. Miret, M. Castilla, and L. de Vicua, "Hierarchical control of intelligent microgrids," *IEEE Industrial Electronics Magazine*, vol. 4, pp. 23–29, Dec 2010.

[2] J. de Matos, F. e Silva, and L. Ribeiro, "Power control in ac isolated microgrids with renewable energy sources and energy storage systems," *IEEE Transactions on Industrial Electronics,*, vol. 62, no. 6, pp. 3490–3498, 2015.

[3] H. Kanchev, D. Lu, F. Colas, V. Lazarov, and B. Francois, "Energy management and operational planning of a microgrid with a pv-based active generator for smart grid applications," *IEEE Transactions on Industrial Electronics*, vol. 58, pp. 4583–4592, Oct 2011.

[4] H. Beltran, E. Bilbao, E. Belenguer, I. Etxeberria-Otadui, and P. Rodriguez, "Evaluation of storage energy requirements for constant production in pv power plants," *IEEE Transactions on Industrial Electronics*, vol. 60, pp. 1225–1234, March 2013.

[5] M.-S. Lu, C.-L. Chang, W.-J. Lee, and L. Wang, "Combining the wind power generation system with energy storage equipment," *IEEE Transactions on Industry Applications*, vol. 45, pp. 2109–2115, Nov 2009.

[6] H. Kakigano, Y. Miura, and T. Ise, "Distribution voltage control for dc microgrids using fuzzy control and gain-scheduling technique," *IEEE Transactions on Power Electronics*, vol. 28, pp. 2246–2258, May 2013.

[7] T. Dragicevic, J. Guerrero, J. Vasquez, and D. Skrlec, "Supervisory control of an adaptive-droop regulated dc microgrid with battery management capability," *IEEE Transactions on Power Electronics*, vol. 29, pp. 695–706, Feb 2014.

[8] I. S. C. C. 21, "Guide for optimizing the performance and life of lead-acid batteries in remote hybrid power systems," *IEEE Std 1561-2007*, pp. C1–25, 2008.

[9] D. Linden and T. Reddy, *Handbook of batteries*. McGraw-Hill handbooks, McGraw-Hill, 2002.

[10] Y.-K. Chen, Y.-C. Wu, C.-C. Song, and Y.-S. Chen, "Design and implementation of energy management system with fuzzy control for dc microgrid systems," *IEEE Transactions on Power Electronics*, vol. 28, pp. 1563–1570, April 2013.

[11] J. Guerrero, J. Vasquez, J. Matas, M. Castilla, and L. de Vicuna, "Control strategy for flexible microgrid based on parallel line-interactive ups systems," *IEEE Transactions on Industrial Electronics*, vol. 56, no. 3, pp. 726–736, 2009.

[12] J. Guerrero, J. Vasquez, J. Matas, L. de Vicua, and M. Castilla, "Hierarchical control of droop-controlled ac and dc microgrids a general approach toward standardization," *IEEE Transactions on Industrial Electronics*, vol. 58, no. 1, pp. 158–172, 2011.

[13] Y. Zhang, H. J. Jia, and L. Guo, "Energy management strategy of islanded microgrid based on power flow control," in *2012 IEEE PES Innovative Smart Grid Technologies (ISGT)*, pp. 1–8, 2012.

[14] X. Lu, K. Sun, J. Guerrero, J. Vasquez, L. Huang, and R. Teodorescu, "Soc-based droop method for distributed energy storage in dc microgrid applications," in *2012 IEEE International Symposium on Industrial Electronics (ISIE)*, pp. 1640–1645, 2012.

[15] C. Li, T. Dragicevic, N. Diaz, J. Vasquez, and J. Guerrero, "Voltage scheduling droop control for state-of-charge balance of distributed energy storage in dc microgrids," in *Energy Conference (ENERGYCON), 2014 IEEE International*, pp. 1310–1314, May 2014.

[16] C. Li, T. Dragicevic, M. Garcia Plaza, F. Andrade, J. Vasquez, and J. Guerrero, "Multiagent based distributed control for state-of-charge balance of distributed energy storage in dc microgrids," in *40th Annual Conference of the IEEE Industrial Electronics Society, (IECON)*, pp. 2180–2184, Oct 2014.

[17] X. Lu, K. Sun, J. Guerrero, J. Vasquez, and L. Huang, "State-of-charge balance using adaptive droop control for distributed energy storage systems in dc microgrid applications," *IEEE Transactions on Industrial Electronics*, vol. 61, pp. 2804–2815, June 2014.

[18] Q. Shafiee, T. Dragicevic, J. Vasquez, and J. Guerrero, "Hierarchical control for multiple dc-microgrids clusters," *IEEE Transactions on Energy Conversion*, vol. 29, pp. 922–933, Dec 2014.

[19] N. Diaz, T. Dragicevic, J. Vasquez, and J. Guerrero, "Intelligent distributed generation and storage units for dc microgrids - a new concept on cooperative control without communications beyond droop control," *IEEE Transactions on Smart Grid*, vol. 5, pp. 2476–2485, Sept 2014.

[20] D. Wu, F. Tang, T. Dragicevic, J. Vasquez, and J. Guerrero, "Autonomous active power control for islanded ac microgrids with photovoltaic generation and energy storage system," *IEEE Transactions on Energy Conversion*, vol. 29, pp. 882–892, Dec 2014.

[21] T. Vandoorn, J. Vasquez, J. De Kooning, J. Guerrero, and L. Vandevelde, "Microgrids: Hierarchical control and an overview of the control and reserve management strategies," *IEEE Industrial Electronics Magazine*, vol. 7, pp. 42–55, Dec 2013.

[22] E. Coelho, P. Cortizo, and P. Garcia, "Small-signal stability for parallel-connected inverters in stand-alone ac supply systems," *IEEE Transactions on Industry Applications*, vol. 38, pp. 533–542, Mar 2002.

[23] V. Salas, E. Olías, A. Barrado, and A. Lázaro, "Review of the maximum power point tracking algorithms for stand-alone photovoltaic systems," *Solar Energy Materials and Solar Cells*, vol. 90, no. 11, pp. 1555 – 1578, 2006.

[24] C. Patsios, A. Chaniotis, M. Rotas, and A. Kladas, "A comparison of maximum-power-point tracking control techniques for low-power variable-speed wind generators," in *8th International Symposium on Advanced Electromechanical Motion Systems Electric Drives Joint Symposium, 2009. ELECTROMOTION 2009*, pp. 1–6, July 2009.

[25] J. Guerrero, L. Garcia De Vicuna, J. Matas, M. Castilla, and J. Miret, "A wireless controller to enhance dynamic performance of parallel inverters in distributed generation systems," *IEEE Transactions on Power Electronics*, vol. 19, pp. 1205–1213, Sept 2004.